Rb and Cs Isotopic Cross Sections from 40-60-MeV-Proton Fission of ^{238}U, ^{232}Th, and ^{235}U

B. L. Tracy,* J. Chaumont, R. Klapisch, J. M. Nitschke, A. M. Poskanzer,†
E. Roeckl,‡ and C. Thibault
Centre de Spectrométrie de Masse du Centre National de la Recherche Scientifique, 91 Orsay, France
(Received 6 August 1971)

The isotopic distributions of Rb and Cs from the fission of ^{238}U, ^{232}Th, and ^{235}U induced by 40- to 60-MeV protons have been measured by means of an on-line mass spectrometer. The Rb isotopic distributions have a Gaussian shape, but those of Cs are somewhat asymmetrical. As the proton bombarding energy increases, the neutron-excess sides of the distributions remain approximately fixed while the neutron-deficient sides shift to lower mass numbers. The distributions also show significant variations with the neutron-to-proton ratio of the target.

All the isotopic cross sections show a significant odd-even structure, with the formation of even neutron isotopes being favored. The effect is more pronounced for the neutron-rich isotopes. A similar structure is found to occur in Rb and Cs distributions from fission induced by thermal neutrons, 155-MeV protons, and 24-GeV protons, as well as in the Na and K cross sections from 24-GeV-proton reactions with a variety of targets. The odd-even effect in the Rb and Cs distributions can be accounted for by a 10 to 15% neutron-pairing effect in the prompt yields and a 2 to 3% pairing effect in the neutron emission.

From the mean mass numbers of the Rb and Cs distributions, the average total number of emitted neutrons has been estimated for each reaction. This information, together with other results on neutron emission as a function of fragment mass, has allowed the mean mass numbers to be corrected for prompt neutron emission. These corrected values differ by about one mass unit from the values predicted by the unchanged-charge-density mechanism and are consistent with the same mechanism of charge division as that operating in thermal-neutron fission.

INTRODUCTION

The usefulness of an on-line mass spectrometer in the study of nuclear-reaction products has been demonstrated in previous publications.[1,2] In the present paper we report the Rb and Cs isotopic cross sections from the fission of ^{238}U, ^{232}Th, and ^{235}U induced by 40- to 60-MeV protons. In connection with the same experiment, the half-lives of the new isotopes $^{98-99}Rb$, ^{98}Sr, and $^{145-146}Cs$ were also measured and are reported elsewhere.[3] Previous cross-section measurements in this energy range have consisted of radiochemical investigations[4-7] of the fission of ^{238}U, ^{232}Th, ^{233}U, ^{239}Pu, and ^{235}U induced by 20- to 85-MeV protons. The on-line mass spectrometer has the advantage of allowing independent-yield measurements of essentially all the isotopes of a given element with a high degree of precision.

Sufficiently precise data can allow the observation of neutron-pairing effects in the isotopic distributions. Several authors have reported the existence of pairing effects in thermal-neutron and spontaneous fission. Thomas and Vandenbosch[8] demonstrated how structure in fragment kinetic energy distributions could be correlated with pairing terms in the mass surface. Wahl, Norris, Rouse, and Williams[9] showed that in the thermal-neutron fission of ^{235}U the yields of even-Z elements are higher than those of odd-Z elements by as much as 40%. These authors found little evidence for a similar dependence of isotonic yields on neutron number, probably because the effect was obscured by neutron emission. Konecny, Gunther, Siegert, and Winter[10] measured independent yields at various values of the fragment kinetic energy in the thermal-neutron fission of ^{235}U. For high kinetic energies they found that the yields of even-even fragments are favored over those of odd-odd fragments. A number of authors[11-13] have observed a pronounced odd-even effect in the cross sections of light products from high-energy nuclear reactions.

Since Rb and Cs are nearly complementary in the fission reactions studied, their isotopic distributions give information on the charge-distribution mechanism at medium energies. It is not clear whether this mechanism is the same as that of low-energy fission, or whether a new process begins to play a role at higher excitation energies. In thermal-neutron and spontaneous fission there is a rearrangement of the nuclear charge such that the heavy fragment has a higher neutron-to-proton ratio than the light fragment. This rearrangement of charge has been described in terms of various models such as equal charge displacement (ECD),[14] minimum potential energy,[15] maximum energy re-

lease,[16] or maximum excitation energy.[17] This same charge-distribution mechanism appears to be valid for excitation energies $\lesssim$20 MeV.[18-20] On the other hand, there is some evidence that at higher excitation energies fission occurs so quickly that the two fragments are left with the same neutron-to-proton ratio as the fissioning parent [unchanged charge density (UCD)]. Colby and Cobble[21] reported that their results from the 20- to 40-MeV ^{4}He-induced fission of ^{233}U, ^{235}U, and ^{238}U were consistent with UCD and inconsistent with ECD. Benjamin, Marsden, Porile, and Yaffe[6] found that their results from the 20- to 85-MeV-proton fission of ^{232}Th and ^{238}U lay between the predictions of UCD and ECD, but closer to UCD. On the other hand, McHugh and Michel[22] obtained results from the ^{4}He-induced fission of ^{232}Th and ^{235}U that were inconsistent with the UCD mechanism.

Briefly, the present investigation was undertaken to study the variations of isotopic distributions with bombarding energy and target. As a result we have obtained information on neutron-pairing effects and the charge-distribution mechanism at medium energies.

EXPERIMENTAL METHOD

A. Mass Spectrometer

The operation of the on-line mass spectrometer has been described in detail elsewhere[1,2,11,23] and only the basic features are given here. In this instrument the target chamber and the ion source are combined in a single unit. The target material is evaporated in the form of a salt onto a number of graphite strips (usually about 20, each measuring 15×4.3 mm^2 in area and 70 μ in thickness). The bundle of graphite strips is then enclosed in a Ta cylinder and the whole assembly is heated up to 2000°C by Joule effect. During an irradiation by a beam of high-energy particles, recoiling reaction products are stopped in the hot graphite. The alkali products diffuse out quickly and are ionized by surface ionization. The ions are then extracted through a slit in the Ta cylinder and analyzed in a conventional mass spectrometer with a 90° sector magnet and a 30-cm radius. Finally the ions pass through a detector slit and are individually counted by means of an electron multiplier. Because of the high diffusion rates and low ionization potentials of the alkali elements, a high degree of chemical selectivity is obtained for these elements.

B. Irradiations

Targets consisting of 1 to 3 mg/cm^2 of ^{238}U, ^{232}Th, and ^{235}U were irradiated in an external proton beam of the Grenoble isochronous cyclotron. Proton bombarding energies used were 40, 50, and 60 MeV. The beam intensity on the target was about 2 μA and this was pulsed to give an irradiation lasting 100 msec every 4.8 sec.

C. Recording of Mass Spectra

A mass range of about four mass units in the Rb region or five mass units in the Cs region was scanned at one time by means of a triangular modulation of the ion accelerating voltage. A rather fast modulation of 40 cps was used because of the rapid diffusion rates of Rb and Cs and because of the time-dependent background between each proton pulse. The mass spectra taken during each scan were stored in a multiscaler memory whose cycling period was synchronized with the high-voltage sweep. The general scheme of irradiation and voltage scanning is shown in Fig. 1. Mass spectra corresponding to two different time intervals in the irradiation cycle were stored in different subgroups of the multiscaler memory. The first spectrum (spectrum A) was recorded during and immediately following the proton beam burst. This spectrum contained most of the independently produced Rb or Cs. The second spectrum (spectrum B) was recorded shortly before the beginning of the next beam burst and contained slowly diffusing Rb or Cs plus any steady-state contribution from cumulative yields and natural contamination. The difference between spectrum A and spectrum B thus yielded directly the relative independent yields.

The spectrum for a certain mass range was recorded over a period of 10 to 30 min in order to accumulate an adequate number of counts. The next mass range was then obtained by changing the magnetic field. There was always at least one mass overlap between one range and the next for normalization purposes. In this way the relative independent yields were obtained for an entire isotopic distribution.

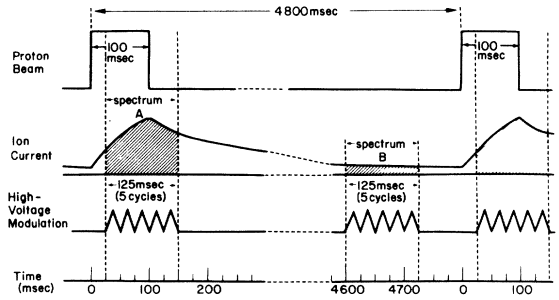

FIG. 1. Scheme of irradiation and scanning. Time zero is the beginning of the proton pulse. The times during which spectra A and B were recorded are indicated by vertical dashed lines.

D. Corrections for Mass Discrimination

The scanning of the accelerating voltage of the mass spectrometer leads to a bias in favor of lighter masses. By means of electrical and magnetic scanning of the same spectrum of stable isotopes, this bias was measured to be $(0.58 \pm 0.05)\%$ for a 1% mass difference, and an appropriate correction was applied to all the experimental data. Any mass discrimination due to differences in recoil ranges of different isotopes was estimated to be less than 2% between the lightest and heaviest isotopes of a given element, and this effect has been neglected in the experimental results.

Throughout the experiment it was assumed that all isotopes of a given element diffuse out of the target at the same rate. In an earlier experiment Chaumont[23] found that any discrimination due to different diffusion rates between ^{83}Rb and ^{89}Rb was less than 2%. However, the fact that the ion current varies nonlinearly during a mass scan leads to a distortion of the mass spectra and consequent errors of 0.5 to 1% in the yield ratios of consecutive isotopes. Corrections for this effect were made from measured diffusion curves, i.e., recordings of the ion current of a stable or long-lived isotope as a function of time after the beam burst (see Ref. 11). Corrections were also made for the radioactive decay of the shortest-lived isotopes during diffusion out of the target.

RESULTS

The independent cross sections for the formation of Rb isotopes are presented in Table I, and those for the formation of Cs isotopes are presented in Table II. The quoted errors indicate the precision of the measurements within a given isotopic distribution. The Rb yields were normalized at mass 86 and the Cs yields at mass 132, 134, 136, and 138 to the radiochemical cross sections of Davies and Yaffe[5] in the case of ^{238}U, and to the data of Benjamin, Marsden, Porile, and Yaffe[6] in the case of ^{232}Th. The Cs yields from ^{235}U were normalized to the measurements of Saha, Tomita, and Yaffe[7] at mass 131, 132, 134, and 136. No Rb cross sections are available for ^{235}U. Since the Rb distributions from ^{235}U and ^{238}U have about the same width, the values in Table I have been normalized so that the area of the distribution from ^{235}U is the same as that from ^{238}U at 50 MeV. All the ^{235}U cross sections have been corrected for the fact that the ^{235}U targets contained 7% ^{238}U. The Cs normalizations at the different mass numbers agreed within the expected errors, and the over-all normalization errors for the Cs cross sections are 8% for ^{238}U, 12% for ^{232}Th, and 9% for ^{235}U. For the Rb normalizations at mass 86, the errors are 29, 28, and 35%, respectively, for ^{238}U at the three energies, and 34% for ^{232}Th.

In some cases it was not possible to measure the

TABLE I. Rb cross sections (mb). Values in parentheses are interpolated. The quoted errors indicate only the precision of the measurements. Normalization errors are given in the text.

A \ Target	^{238}U	^{238}U	^{238}U	^{232}Th	^{235}U [a]
p energy	40 MeV	50 MeV	60 MeV	50 MeV	50 MeV
85				0.06 ±0.03	0.34 ±0.02
86	0.070±0.003	0.150±0.012	0.30 ±0.08	0.30 ±0.03	0.84 ±0.02
87	(0.433)	(1.03)	(2.03)	1.43 ±0.06	(3.06)
88	1.69 ±0.02	3.16 ±0.06	5.27 ±0.28	4.52 ±0.08	7.38 ±0.06
89	3.32 ±0.02	7.45 ±0.07	10.78 ±0.13	8.77 ±0.06	12.97 ±0.07
90	6.26 ±0.03	12.65 ±0.08	17.42 ±0.15	12.84 ±0.06	16.36 ±0.07
91	9.09 ±0.03	17.75 ±0.09	22.38 ±0.15	14.51 ±0.06	17.00 ±0.07
92	8.77 ±0.03	16.04 ±0.08	20.12 ±0.13	10.80 ±0.11	11.83 ±0.10
93	6.85 ±0.04	12.19 ±0.10	14.92 ±0.15	6.39 ±0.07	6.80 ±0.07
94	3.34 ±0.02	5.91 ±0.06	7.31 ±0.08	2.35 ±0.04	2.36 ±0.04
95	1.51 ±0.01	2.67 ±0.03	3.28 ±0.05	0.89 ±0.02	0.76 ±0.02
96	0.419±0.006	0.758±0.011	(1.16)	0.210±0.008	0.215±0.009
97	0.117±0.002	0.210±0.004	0.27 ±0.02	0.054±0.005	0.052±0.005
98	0.014±0.001	0.028±0.001	0.06 ±0.02		
Total	41.88	80.00	105.86	63.12	80.00
$\langle A \rangle$	91.511±0.003	91.402±0.005	91.295±0.013	90.747±0.007	90.425±0.006
Width [b]	1.818±0.002	1.826±0.004	1.925±0.010	1.762±0.006	1.833±0.003

[a] Normalized to give the same area as the Rb distribution from ^{238}U at 50 MeV.
[b] Standard deviation of the distribution.

independent yields of Rb at mass 87 and of Cs at mass 133, 135, and 137. This was due to high cumulative yields at these masses and anomalous enhanced diffusion of the cumulative components during proton irradiation. The problem was most serious for the ^{238}U target, which had had a long history of irradiation and thus had accumulated large amounts of Rb and Cs at these masses. This difficulty did not occur at other masses, where the cumulative yields are much lower and where the half-lives of the alkalis are much shorter. The values enclosed in parentheses in Tables I and II have been interpolated or extrapolated from smooth curves drawn through the data points. These values were needed to allow integration of the total distributions.

For each distribution Tables I and II show the total elemental cross section along with mean mass number $\langle A \rangle$ and the "width" or standard deviation of the distribution. The errors in the quantities $\langle A \rangle$ and "width" depend only on the precision of the mass-spectrometric measurements, and hence are very small.

The Rb distributions from ^{238}U at the three bombarding energies are shown in Fig. 2, and from the three targets at a bombarding energy of 50 MeV in Fig. 3. The distributions are quite symmetrical, and it was found that they could be well represented by Gaussian curves. The Cs distributions from ^{238}U at the three bombarding energies are shown in Fig. 4, and from the three targets at a bombarding energy of 50 MeV in Fig. 5. These distributions are broader and decidedly less symmetrical than those of Rb. In particular, the Cs distributions have a pronounced shoulder on the heavy-mass side.

Variations with Bombarding Energy

Even over the narrow energy range of 40 to 60 MeV, there is a distinct energy dependence. In Fig. 4 it is apparent that, as the bombarding energy increases, the heavy-mass side of the Cs distributions remains approximately fixed, while the light-mass side shifts downward toward more neutron-deficient isotopes. In Fig. 2, the cross sections of the neutron-deficient Rb isotopes increase more rapidly with bombarding energy than those of the neutron-rich isotopes, and there is a net displacement of the centers of the distribution to lower mass numbers.

These trends can be expressed more quantitatively in terms of the mean mass numbers $\langle A \rangle$ and standard deviations of the distributions. In Fig. 6 the quantities $(\langle A \rangle - Z)/Z$, which are the average neutron-to-proton ratios of the isotopic distributions, are plotted as functions of bombarding energy for ^{238}U fission and ^{232}Th fission. Figure 7

TABLE II. Cs cross sections (mb). Values in parentheses are interpolated or extrapolated. The quoted errors indicate only the precision of the measurements. Normalization errors are given in the text.

A \ Target	^{238}U	^{238}U	^{238}U	^{232}Th	^{235}U
p energy	40 MeV	50 MeV	60 MeV	50 MeV	50 MeV
130					0.11 ±0.02
131	0.032 ± 0.006	0.09 ±0.01	(0.35)		0.93 ±0.04
132	0.177 ± 0.008	0.56 ±0.03	1.04 ±0.12	0.45 ±0.04	3.11 ±0.08
133	(0.950)	(2.35)	(3.50)	1.41 ±0.08	7.92 ±0.16
134	3.27 ±0.05	6.50 ±0.09	8.58 ±0.04	4.78 ±0.18	13.0 ±0.2
135	(8.54)	(15.0)	(16.6)	11.8 ±0.3	18.9 ±0.3
136	17.24 ±0.11	24.4 ±0.2	23.6 ±0.5	18.9 ±0.2	19.2 ±0.3
137	(21.50)	(27.4)	(25.9)	(21.8)	20.7 ±0.3
138	22.52 ±0.19	22.8 ±0.3	21.2 ±0.8	21.2 ±0.4	14.7 ±0.3
139	20.53 ±0.12	19.6 ±0.4	16.9 ±0.4	14.8 ±0.3	7.47 ±0.18
140	14.30 ±0.15	13.4 ±0.3	11.9 ±0.4	9.0 ±0.3	4.56 ±0.16
141	9.56 ±0.11	10.1 ±0.2	8.8 ±0.3	5.9 ±0.2	2.70 ±0.10
142	4.19 ±0.06	4.89 ±0.13	4.6 ±0.2	2.45 ±0.12	1.00 ±0.05
143	1.98 ±0.05	2.54 ±0.06	2.5 ±0.2	1.06 ±0.09	0.30 ±0.05
144	0.360 ± 0.017	0.72 ±0.03	(1.1)	(0.30)	0.04 ±0.02
145	0.113 ± 0.008	0.20 ±0.02	(0.5)		
146	0.031 ± 0.007				
Total	127.00	150.0	146.5	113.8	114.6
$\langle A \rangle$	138.056 ± 0.011	137.680 ± 0.014	137.491 ± 0.024	137.504 ± 0.015	136.231 ± 0.013
Width [a]	2.099 ± 0.009	2.266 ± 0.009	2.413 ± 0.015	2.062 ± 0.010	2.198 ± 0.008

[a] Standard deviation of the distribution.

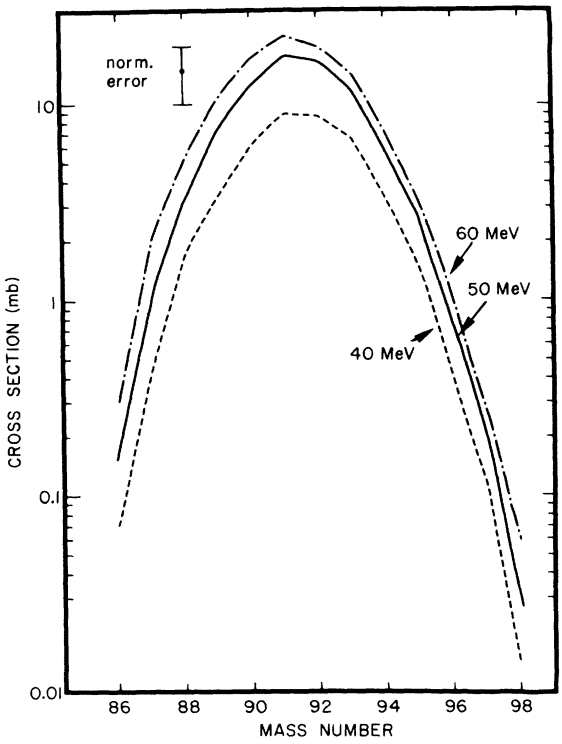

FIG. 2. Rb distributions from the fission of ^{238}U by 40-, 50-, and 60-MeV protons.

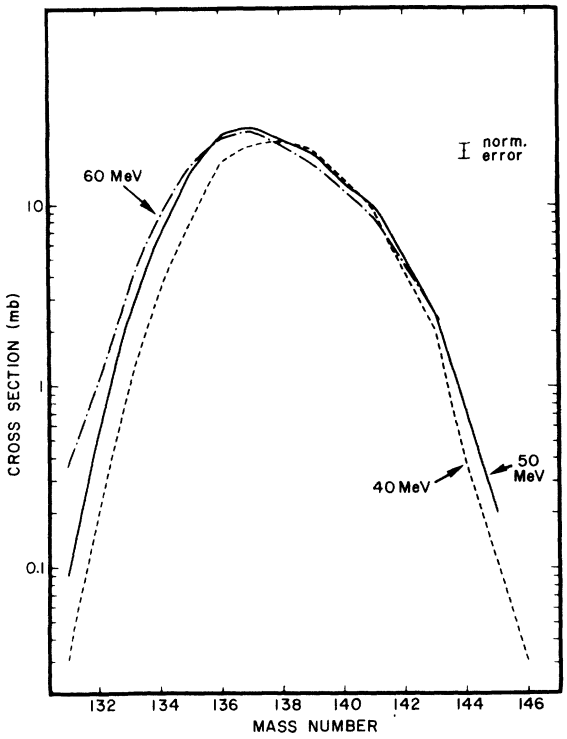

FIG. 4. Cs distributions from the fission of ^{238}U by 40-, 50-, and 60-MeV protons.

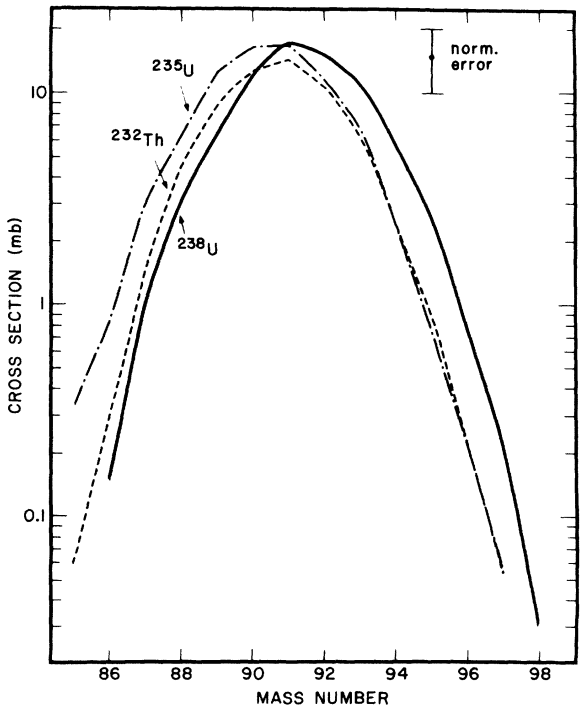

FIG. 3. Rb distributions from the fission of ^{238}U, ^{232}Th, and ^{235}U by 50-MeV protons.

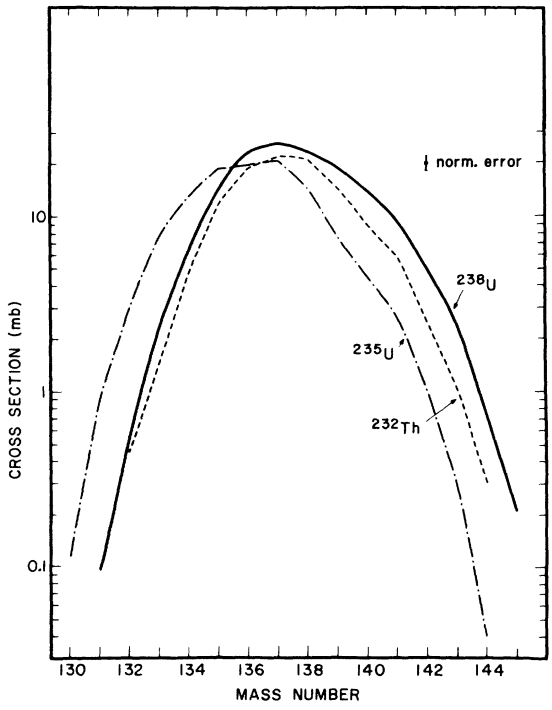

FIG. 5. Cs distributions from the fission of ^{238}U, ^{232}Th, and ^{235}U by 50-MeV protons.

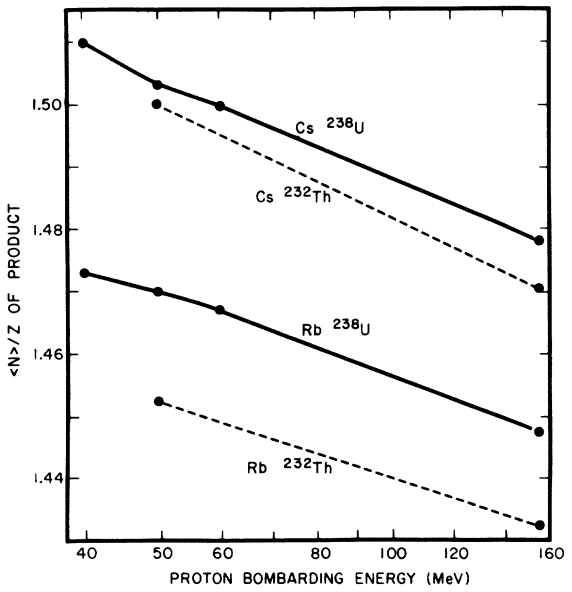

FIG. 6. Average N/Z ratios of the Rb and Cs distributions from the fission of ^{238}U and ^{232}Th as a function of the logarithm of proton bombarding energy. The error bars are smaller than the size of the experimental points.

shows the widths as functions of bombarding energy for the same fission reactions. The results for the 155-MeV-proton fission of ^{238}U and ^{232}Th were taken from the work of Chaumont,[23] and are shown in these two graphs for comparison. From Figs. 6 and 7, it is apparent that an increase in bombarding energy is associated with a downward shift in the average N/Z ratios and an increase in the

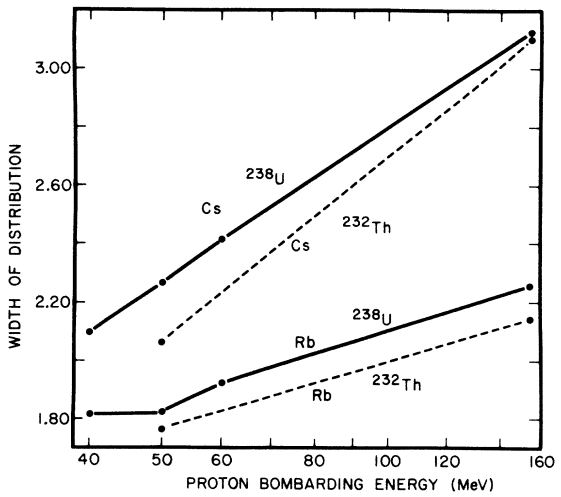

FIG. 7. The widths, expressed as standard deviations, of the Rb and Cs distributions from the fission of ^{238}U and ^{232}Th as a function of the logarithm of proton bombarding energy. The error bars are smaller than the size of the experimental points.

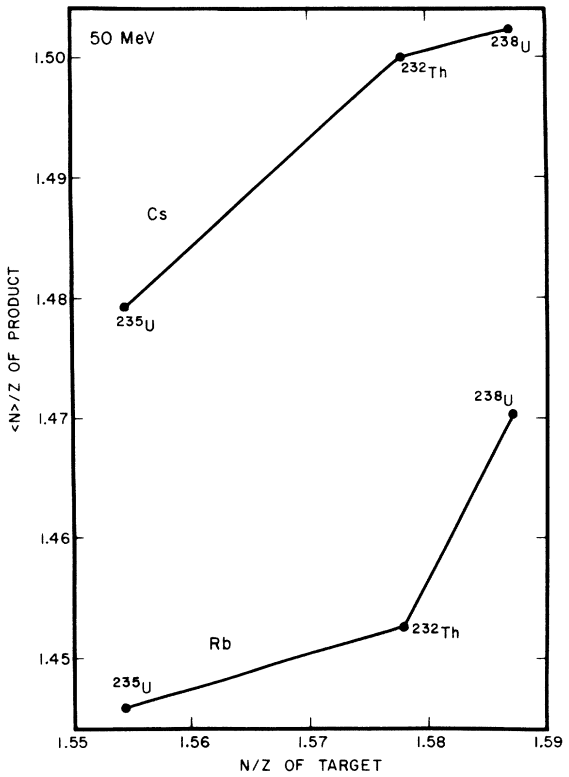

FIG. 8. Average N/Z ratios of the Rb and Cs distributions from 50-MeV-proton fission as a function of the N/Z ratio of the target. The error bars are smaller than the size of the experimental points.

widths of the distributions. Yaffe[4] has reported an analogous shift of the most-probable charge towards stability, and a broadening of charge-distribution curves with increasing bombarding energy in the range 20 to 85 MeV.

Two further observations are worth noting here. First of all, there is a considerable gap in Fig. 6 between the N/Z ratios of Cs distributions and those of Rb distributions, with the Cs distributions being more neutron rich. The magnitude of this gap does not appear to change with energy. Secondly, in thermal-neutron fission, the Rb and Cs distributions both have the same standard deviation[23] of 1.52 ± 0.03 mass units. However, it is apparent from Fig. 7 that the Cs distributions broaden much more quickly with increasing bombarding energy.

Variations with Target

In Figs. 3 and 5 the distributions from ^{235}U fission have about the same width as those from ^{238}U fission, but are shifted to lower mass numbers. On the other hand, the distributions from ^{232}Th fission are distinctly narrower than those from ^{238}U. This narrowness is also evident in Fig. 7. In Fig.

8 the average neutron-to-proton ratios of the product distributions at a bombarding energy of 50 MeV are plotted as a function of the N/Z ratios of the targets. It is clear that a more neutron-rich target leads to more neutron-rich products. However, the relationship is far from being linear as one might at first expect. The average N/Z ratio of Rb from ^{232}Th is too low, and that of Cs from ^{232}Th is too high. Hence it would be unwise to make interpolations for other fissioning nuclei from this type of graph. All three targets show a wide gap between the average N/Z ratios of Cs distributions and those of Rb distributions.

Odd-Even Effect

It is already apparent in Figs. 2 to 5 that there is a slight odd-even structure in the Rb and Cs cross sections, particularly for the neutron-rich isotopes. The tendency is for the yields of the even-neutron (odd-mass) isotopes to be favored. In order to make this structure more evident we shall employ a method of differences. Let L_0, L_1, L_2, and L_3 be the natural logarithms of the relative isotopic yields at the mass numbers A, $A+1$, $A+2$, and $A+3$. We then define the third difference for this mass interval as:

$$D_3 \equiv \tfrac{1}{8}(-1)^A[(L_3 - L_0) - 3(L_2 - L_1)]\,. \qquad (1)$$

If L_0 to L_3 lie on a parabola (i.e., the data are Gaussian) then it is easily shown that the third difference is exactly zero. Suppose now that the logarithms of the yields of odd-mass isotopes all lie above a smooth parabola by an amount Δ, and those of even-mass isotopes all lie below this curve by an equal amount. Then, starting with a mass interval where A is even, we replace L_0 by $L_0 - \Delta$, etc. in Eq. (1) and the third difference becomes

$$D_3 = \tfrac{1}{8}(-1)^A\{[(L_3 + \Delta) - (L_0 - \Delta)] - 3[(L_2 - \Delta) - (L_1 + \Delta)]\} = +\Delta\,.$$

For the next consecutive mass interval, which starts at $A+1$, the third difference will also be $+\Delta$.

Thus if the yields of odd-mass isotopes are favored, the third differences will be consistently greater than zero and will yield directly the average fractional odd-even effect for each interval of four masses. In this treatment, it is not necessary to assume that the logarithms of the yields are best fitted by a parabolic curve. If the "best" curve were to have a finite third derivative, then the third differences would show regular oscillations because of the $(-1)^A$ term. Corrections could easily be made for such an effect. The resulting third differences for all Rb distributions are shown in Fig. 9, and those for all Cs distributions are shown in Fig. 10. The experimental data of Chaumont[23] have been used to compute the third differences from fission by thermal neutrons, 155-MeV protons, and 24-GeV protons. From these graphs it is evident that a small but significant odd-even effect exists in all of the Rb and Cs isotopic distributions measured up to the present. This effect varies more or less smoothly with mass number, but shows no apparent dependence on target or bombarding energy. The effect is 10% or higher

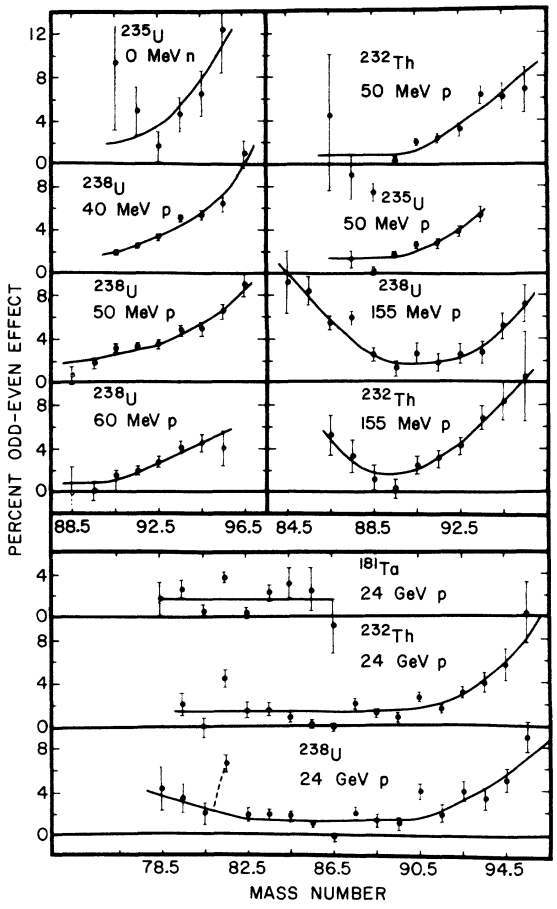

FIG. 9. Percent odd-even effect in the Rb distributions. The third difference for each mass interval A to $A+3$ is plotted at the midpoint of this interval, i.e., at mass $A+1.5$. In each case a smooth curve has been drawn by eye through the computed points. Open circles represent third differences containing one or more interpolated or extrapolated yields. These points have been given less weight when drawing the smooth curve. In some cases, points with poor statistics near the edges of the distributions have been omitted. In the case of ^{232}Th + 50 MeV p, the point at mass 88.5 does include a measurement for ^{87}Rb. However, even a slight influence on this measurement from the enhanced diffusion effect would show up dramatically on the third difference. For that reason one cannot draw any conclusion from the anomalous value that appears at this mass.

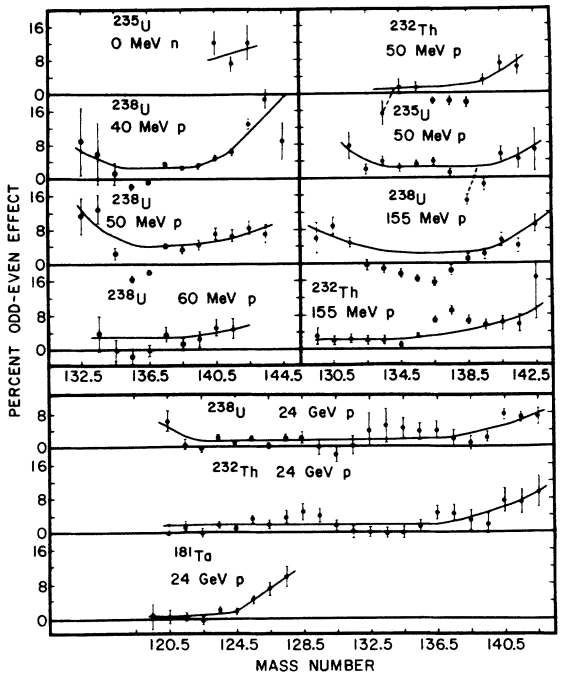

FIG. 10. Percent odd-even effect in the Cs distributions. See the caption of Fig. 9. Same remark as above concerning the anomalous value at mass 138.5 for ^{235}U +50 MeV p.

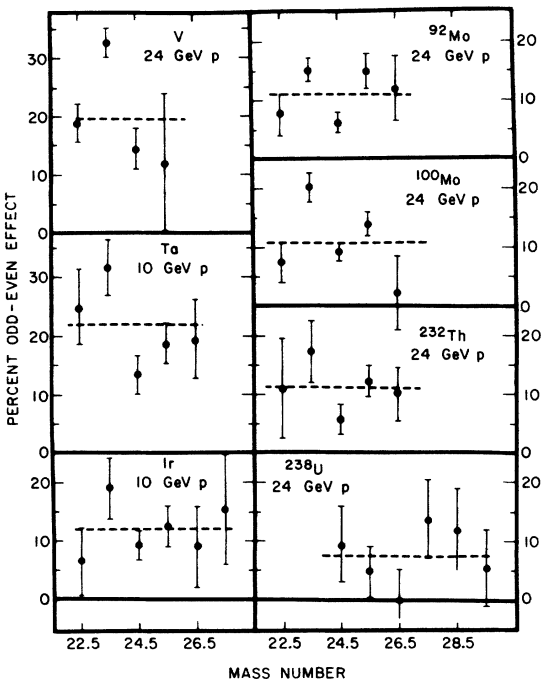

FIG. 12. Percent odd-even effect in Na distributions. As before, the third difference for each mass interval A to $A+3$ is plotted at $A+1.5$. The dashed lines indicate the unweighted averages in each case.

for the most neutron-rich isotopes, but levels off to a value of about 2% near the maxima of the distributions. Some graphs show a tendency to increase on the neutron-deficient side, but this is not reproduced in all cases.

Figure 11 shows the third differences for the K distributions measured for 24-GeV-proton reactions by Chaumont.[23] The odd-even effect, particularly in the case of the Ta target, shows a behavior similar to that of the Rb and Cs distributions.

Figure 12 shows the third differences for the Na distributions measured for 10- and 24-GeV-proton reactions by Thibault.[11] Here the odd-even effect is much larger, but shows no obvious mass dependence. The dashed line on each graph indicates the unweighted average of the third differences. This average varies from 10 to 20%. There is an oscillation of points about the average values which probably results from the fact that the Na isotopic distributions are narrow and that the effect of the third derivative is significant over a range of four masses.

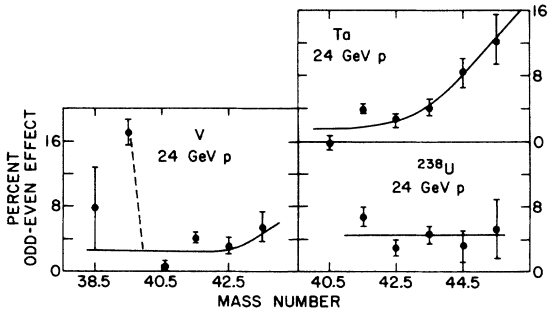

FIG. 11. Percent odd-even effect in K distributions. See the caption of Fig. 9. The dashed line on the graph for the V target indicates an anomalously high value at 39.5, undoubtedly caused by natural K contamination.

DISCUSSION

A. Cascade-Evaporation Model

Although it is questionable whether Monte Carlo cascade calculations make accurate predictions for incident proton energies in the range of 40 to 60 MeV, certain features of the isotopic distributions can be understood, at least qualitatively, in terms of a prompt nuclear cascade followed by particle evaporation. We have adapted a Monte Carlo cascade calculation originally developed by Cohen,[24] to this energy region. It predicts a strong component of compound-nuclear events (35 to 60% of all events) in which the nucleus receives the maximum possible excitation energy. In addition, (p, xn) cascade events lead to a spectrum of excitation energies which extends down to zero. The persistence

of these low deposition energy events could explain why the neutron-rich side of the isotopic distributions remains more or less fixed with increasing bombarding energy. On the other hand, the progressively higher excitation energies available with increasing bombarding energy lead to greater neutron evaporation, and hence to increasingly higher yields of neutron-deficient isotopes. Thus the isotopic distributions appear to broaden toward lower masses as the bombarding energy increases.

Furthermore, if we assume that for each excitation energy the center of the isotopic distribution is proportional to the atomic number of the element, then the broadening of the Cs distributions due to the spread in excitation energies should be 55/37 times greater than the broadening of the Rb distributions. We do observe greater widths for the Cs distributions although the factor 55/37 does not appear to be exactly reproduced. It is possible that the broader valley of β stability in the Cs region also plays a role in the greater widths of the Cs distributions.

B. Analysis of Odd-Even Effect

An odd-even effect which favors even-neutron species in the isotopic distribution could have two possible origins:
(1) a preference in the nuclear division itself for fragments with even numbers of neutrons, because of the higher Q values involved;
(2) a tendency for odd-neutron prompt fragments to evaporate slightly more neutrons than even-neutron prompt fragments.

In the first case, neutron emission from the prompt fragments will tend to smear out any structure originally present at the moment of scission. However, this structure will tend to be preserved on the neutron-rich side of the isotopic distribution. This is because the yields of the neutron-rich fragments are decreasing very quickly with increasing neutron number, and neutron evaporation from higher-mass isotopes has very little effect on the observed yield of the isotope at mass A. Expressed differently, the observed yields of the neutron-rich isotopes result from events in which very few if any neutrons are emitted. On the other hand, near the maximum of the isotopic distribution, the yields of adjacent isotopes are about equal, and neutron emission from higher-mass isotopes becomes more effective in smearing out pairing structure. The mass dependence of the observed odd-even effects reported here would seem to support the first case as the origin of the pairing structure. In the second case, a pairing effect in the neutron emission leads to a structure which is nearly constant with mass.

On the basis of the first case, a preliminary calculation has been performed of the odd-even effect in the Rb distribution from ^{238}U at 50 MeV. An original pairing effect of constant magnitude was assumed with respect to a smooth prompt curve which was chosen so as to reproduce a Gaussian fit to the observed yields after neutron emission had been taken into consideration. The probability P_n of emitting n neutrons was assumed to be the same for all isotopes, and to be given by the Poisson law

$$P_n = \frac{\nu^n}{n!} e^{-\nu},$$

where ν is the average number of emitted neutrons from the Rb fragments. From the structured prompt yields and the assumed neutron-distribution function the secondary yields were calculated and then analyzed by the third-difference formula. Taking $\nu = 1.6$ from Table III, we obtain the solid curve in Fig. 13 for an effect $\Delta = \pm 18\%$ in the prompt yields. This calculation reproduces the general trend in the observed odd-even effect in

TABLE III. Number of emitted neutrons and charge-distribution mechanism.

Target	^{238}U	^{238}U	^{238}U	^{232}Th	^{235}U
p energy	40 MeV	50 MeV	60 MeV	50 MeV	50 MeV
ν_T	7.00 ± 0.04	7.53 ± 0.06	7.86 ± 0.09	7.33 ± 0.06	6.98 ± 0.06
ν_C	0.35	0.51	0.60	0.50	0.51
ν_E	$2.06^{+1.6}_{-1.4}$	$2.16^{+1.8}_{-1.5}$	$2.70^{+1.5}_{-2.0}$	$2.19^{+1.6}_{-0.9}$	$1.83^{+1.4}_{-1.5}$
ν_L	1.53	1.62	1.52	1.55	1.55
ν_H	3.06	3.24	3.04	3.09	3.09
$\langle A'(\mathrm{Rb})\rangle$	93.04	93.02	92.82	92.30	91.97
$\langle A'(\mathrm{Cs})\rangle$	141.12	140.92	140.53	140.59	139.32
ΔA(Rb)	−1.10 ± 0.16	−1.03 ± 0.16	−0.99 ± 0.16	−1.37 ± 0.16	−1.01 ± 0.15
ΔA(Cs)	+1.19 ± 0.16	+1.12 ± 0.16	+1.09 ± 0.16	+1.36 ± 0.16	+1.11 ± 0.15
ΔZ(Rb)	+0.44 ± 0.06	+0.41 ± 0.06	+0.40 ± 0.06	+0.55 ± 0.06	+0.40 ± 0.06
ΔZ(Cs)	−0.48 ± 0.06	−0.45 ± 0.06	−0.44 ± 0.06	−0.54 ± 0.06	−0.44 ± 0.06

the region of high masses, but descends too quickly to zero and fails to account for the 2 to 3% effect near the yield maximum. A more satisfactory result is obtained by assuming a mixture of the first and second cases. The Poisson distribution was slightly modified to allow a ±2.5% variation in P_n, depending on whether the emission of n neutrons left the final nucleus with an even or odd total number of neutrons. The dashed curve in Fig. 13 shows the results of this calculation with $\Delta = \pm 12\%$ in the prompt yields.

It is possible that the Poisson law does not give a realistic distribution of the number of neutrons emitted. A more exact calculation would make use of neutron-evaporation theory and an appropriate distribution of excitation energies for each isotope. However, the precision of the third differences computed from the experimental data probably does not justify a more detailed analysis at this time. In conclusion we feel that there is a 10 to 15% neutron pairing effect in the Rb and Cs prompt yields and probably also a 2 to 3% pairing effect in the neutron emission. We do not yet understand the apparent increase in the odd-even effect toward the neutron-deficient yields in some cases.

C. Total Number of Neutrons Emitted

From the $\langle A \rangle$ values in Tables I and II it is possible to calculate the average total number of emitted neutrons, at least for the mass divisions studied, for each combination of target and bombarding energy. This analysis is somewhat complicated by the fact that Rb and Cs are not exactly complementary products as happened to be the case in the thermal-neutron fission of ^{235}U.[23] However, in the energy range of 40 to 60 MeV the probability of charged-particle emission is small; nearly all of the events are of the compound-nucleus or of the (p, xn)-cascade type. Thus in the case of uranium targets the fissioning nucleus is almost certainly some isotope of neptunium, and in the case of thorium targets some isotope of protactinium.

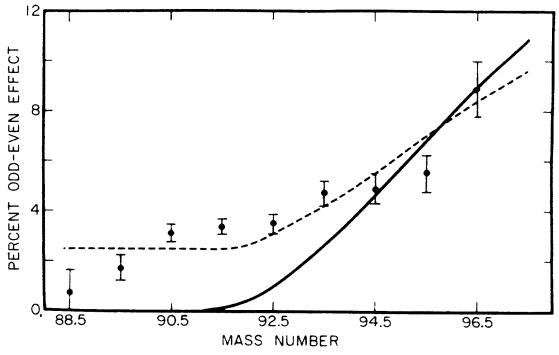

FIG. 13. Analysis of the odd-even effect in the Rb distribution from the fission of ^{238}U by 50-MeV protons. The points are computed from the experimental data, and are the same as in Fig. 9. The solid curve shows the results of the calculation for $\nu = 1.6$, $\Delta = \pm 18\%$, and no pairing effect in neutron emission; and the dashed curve for $\nu = 1.6$, $\Delta = \pm 12\%$, and a ±2.5% effect in neutron emission.

If the fissioning nucleus is Np, then the complement of a Rb fragment is a Ba fragment, and that of a Cs fragment is one of Sr. Furthermore, since Ba is only one charge unit removed from Cs, the mean mass number of Ba fragments can be estimated as follows:

$$\langle A(\mathrm{Ba}) \rangle = \tfrac{56}{55} \langle A(\mathrm{Cs}) \rangle ; \tag{2}$$

similarly, we have

$$\langle A(\mathrm{Sr}) \rangle = \tfrac{38}{37} \langle A(\mathrm{Rb}) \rangle . \tag{3}$$

This gives two expressions for ν_T, the total number of neutrons emitted both before and after fission:

$$\nu_T = A_0 + 1 - \langle A(\mathrm{Rb}) \rangle - \tfrac{56}{55} \langle A(\mathrm{Cs}) \rangle$$

and

$$\nu_T = A_0 + 1 - \langle A(\mathrm{Cs}) \rangle - \tfrac{38}{37} \langle A(\mathrm{Rb}) \rangle ,$$

where A_0 is the mass number of the target nucleus. The resulting ν_T values from the two expressions agree to within 0.04 neutrons. The two results are averaged to give the number of emitted neutrons for a mass ratio of about 1.5. A similar procedure is followed for the ^{232}Th target, except that Rb is now paired with Xe, and Cs with Kr. The first line of Table III shows the resulting ν_T value for each combination of target and bombarding energy.

A small error is introduced in expressions (2) and (3) because the UCD mechanism is not strictly valid (see next section), and hence the mean mass number for each element is not exactly proportional to the nuclear charge. However, the errors go in opposite directions for the light and heavy fragments and thus tend to cancel in the average value of ν_T. A second small error occurs because the number of prompt neutrons increases with fragment mass and, for example, is higher for the mass $\langle A(\mathrm{Ba}) \rangle$ than for $\langle A(\mathrm{Cs}) \rangle$. This leads to an estimated correction of +0.05 neutrons, which has been applied to the ν_T values in Table III. Finally, a small correction has been applied because of the finite probability of emitting protons during the prompt cascade. The number of cascade protons varies from 0.01 per fission event at 40 MeV to 0.05 per fission event at 60 MeV, according to the Monte Carlo calculation of Sec. A. The quoted errors in the ν_T values of Table III include the uncertainties in these corrections.

D. Charge-Distribution Mechanism

The wide gap between the N/Z ratios of the Cs and the Rb distributions evident in Figs. 6 and 8 already indicates that the UCD mechanism may not be valid in fission at these energies. However, before conclusions can be drawn about the charge-distribution mechanism in proton-induced fission at these energies, the average fissioning nucleus must be determined and the mean mass numbers of the Rb and Cs isotopic distributions must be corrected for post-fission neutron emission. If the small contribution from proton emission is neglected, then the mass of the fissioning nucleus is

$$A_F = A_0 + 1 - (\nu_C + \nu_E), \tag{4}$$

and its nuclear charge is

$$Z_F = Z_0 + 1, \tag{5}$$

where A_0 and Z_0 are the mass and charge of the target nucleus, ν_C is the number of neutrons per fission event emitted during the prompt cascade, and ν_E is the number of neutrons evaporated before fission. The number ν_C has been estimated from the Monte Carlo calculations of Sec. A and is shown in Table III for each combination of target and bombarding energy. The calculation of the number ν_E begins with the spectrum of cascade products and assumes that each evaporated neutron carries off an amount of excitation energy equal to its binding energy plus 2-MeV kinetic energy. The fission-width-to-neutron-emission-width ratios, Γ_f/Γ_n, are calculated by means of a statistical model,[25] and the resulting values of ν_E are given in Table III. The lower limits in ν_E are obtained by using instead the Γ_f/Γ_n values of Vandenbosch and Huizenga,[26] who assume that Γ_f/Γ_n is independent of excitation energy. However, Cheifetz *et al.*[27] find better agreement with their neutron-emission measurements in 155-MeV-proton fission by means of the same statistical model used here. This model predicts that Γ_f/Γ_n decreases with increasing excitation energy. The upper limits in ν_E are obtained by assuming that only three of the total number of neutrons ν_T are emitted after fission. (Even in the thermal-neutron fission of ^{235}U, 2.5 neutrons are emitted after fission.) We shall eventually show that the final results are insensitive to these possible variations in ν_E. However, it is necessary to keep three significant figures throughout Table III in order to show that the errors cancel.

The numbers of neutrons ν_L and ν_H emitted after fission from the light and heavy fragments, respectively, must now be determined. The sum of these quantities is given by

$$\nu_L + \nu_H = \nu_T - (\nu_C + \nu_E), \tag{6}$$

where ν_T has been estimated in Sec. C. Furthermore, the ratio ν_H/ν_L can be interpolated from existing experimental data. In the 12-MeV-proton fission of ^{238}U, Cheifetz and Fraenkel[28] find $\nu_H/\nu_L \sim 1.5$ for a mass ratio of 1.5, i.e., the approximate ratio of the masses of Cs and Rb fragments. Cheifetz *et al.*[27] find that ν_H/ν_L increases to about 2.2 for the same mass ratio in the 155-MeV-proton fission of ^{238}U. The measurements of Britt and Whetstone[29] on the 30-MeV ^{4}He-induced fission of ^{233}U indicate $\nu_H/\nu_L \sim 1.7$ for this mass ratio. We are thus led to assume a value of 2.0 ± 0.3 in 40- to 60-MeV proton-induced fission. The resulting values of ν_L and ν_H are shown in Table III along with $\langle A'(\mathrm{Rb})\rangle$ and $\langle A'(\mathrm{Cs})\rangle$, the mean mass numbers of the prompt Rb and Cs isotopic distributions, i.e., the experimental mean masses corrected for post-fission neutron emission. Since our experimental data consist of isotopic rather than isobaric distributions, we have chosen to calculate the most-probable mass for a given element rather than to follow the conventional procedure of calculating the most-probable charge at a given mass number. The prediction of UCD for the most-probable prompt mass of an element with atomic number Z is

$$A'_{\mathrm{UCD}}(Z) = (Z/Z_F)A_F = \frac{Z}{Z_0+1}[(A_0+1) - (\nu_C + \nu_E)], \tag{7}$$

where A_F and Z_F have been substituted from expressions (4) and (5).

In Table III the rows titled $\Delta A(\mathrm{Rb})$ and $\Delta A(\mathrm{Cs})$ indicate the differences between the mean prompt masses $\langle A'(Z)\rangle$ and the UCD predictions $A'_{\mathrm{UCD}}(Z)$. The quoted errors in the differences result from the uncertainty of ± 0.3 in the ratio ν_H/ν_L. If the upper or the lower limits on the ν_E values are taken instead of the central values, then the resulting differences still fall within the range of their quoted errors. The reason for this is that the quantities $\langle A'(Z)\rangle$ and $A'_{\mathrm{UCD}}(Z)$ both contain ν_E [see expressions (6) and (7)], and that the errors in ν_E tend to cancel when the difference is taken between $\langle A'(Z)\rangle$ and $A'_{\mathrm{UCD}}(Z)$. It is apparent that all the mean prompt mass numbers of the Rb distributions are lower than the UCD predictions, and that the mean prompt mass numbers of the Cs distributions are higher by about the same amount. The average difference from UCD for the fission of the uranium isotopes is about 1.10 mass units, and that for the fission of ^{232}Th is about 1.4. In order to obtain agreement with UCD in case of uranium fission, it would be necessary to add 1.10 neutrons to ν_L and to subtract the same number from ν_H. This would give a ratio $\nu_H/\nu_L \sim 0.8$,

which is inconsistent with all the experimental measurements of ν as a function of fragment mass in the medium-energy region.

In the thermal-neutron fission of ^{235}U Chaumont[23] has found -1.16 ± 0.11 and $+1.15 \pm 0.14$ mass units, respectively, for the differences between the mean prompt masses of the Rb and Cs distributions and the UCD predictions. These values are in excellent agreement with our mass differences in the 40- to 60-MeV-proton fission of uranium isotopes. The mass differences ΔA(Rb) and ΔA(Cs) have been converted to charge differences by multiplying by 0.4, the average charge-to-mass ratio, and are shown as ΔZ(Rb) and ΔZ(Cs) in Table III. The results for the fission of the uranium isotopes vary between 0.4 and 0.5, which agree well with the average charge differences obtained from the thermal-neutron fission of ^{235}U by radiochemical[9] and by physical[30,31] methods. As one final comparison, we have carried out calculations for the fission of ^{238}U by 50-MeV protons based on the assumption of ECD,[14] which has enjoyed considerable success in thermal-neutron fission. First of all, the most-probable charges were calculated by ECD for the mean prompt masses of the Rb and Cs distributions. These most-probable charges were then compared with the UCD predictions, and the differences, $Z_p^{\mathrm{ECD}} - Z_p^{\mathrm{UCD}}$, were +0.36 for Rb and −0.32 for Cs. These values are in reasonable agreement with $+0.41 \pm 0.06$ and -0.45 ± 0.06 obtained for this reaction in Table III. ECD calculations for the other reactions studied give similar results. In particular, there is no tendency for the experimental results to lie between the UCD and ECD predictions as some authors have suggested.[4,6,21]

It must be pointed out that conclusions on the charge-distribution mechanism at these energies are sensitive to assumptions made about the division of excitation energy between the light and heavy fragments. Colby and Cobble,[21] as well as Benjamin, Marsden, Porile, and Yaffe,[6] assumed that the excitation energy is divided in proportion to the fragment masses; whereas the recent neutron-emission measurements[27-29] would indicate that the heavy fragment receives even more than its share of the excitation energy on a proportionality basis. These authors were thus led to underestimate the number of neutrons emitted from the heavy fragments and, since their measurements were mainly concerned with heavy fragments, they obtained results which lay closer to the UCD predictions.

In this paper we are led to conclude that the charge-distribution mechanisms operating in thermal-neutron fission can account equally well for the Rb and Cs cross sections in 40- to 60-MeV-proton fission. This conclusion is based on our precise independent-yield measurements of both light and heavy fragments, as well as on the most recent measurements of neutron emission as a function of fragment mass.

ACKNOWLEDGMENTS

The authors gratefully acknowledge the stimulation and incentive given to us by the late René H. Bernas who led us into the field of on-line mass spectrometry. We thank Professor J. Yoccoz, Professor J. Valentin, and their colleagues from the Institut des Sciences Nucléaires whose support made this experiment possible at the Grenoble cyclotron. We also acknowledge the excellent assistance of Fermé and the cyclotron crew and we are grateful to R. Fergeau, M. Jacotin, and G. Le Scornet for their able technical assistance during the course of this experiment.

---

*National Research Council of Canada, Postdoctoral Fellow.

†Guggenheim Fellow, Permanent address: Lawrence Radiation Laboratory, Berkeley, California.

‡Research Associate KFA-JULICH-Germany.

[1]R. Klapisch, J. Chaumont, J. Jastrzebski, R. Bernas, G. N. Simonoff, and M. Lagarde, Phys. Rev. Letters 20, 743 (1968). See also R. Klapisch, Ann. Rev. Nucl. Sci. 19, 33 (1969).

[2]R. Klapisch, J. Chaumont, C. Philippe, I. Amarel, R. Fergeau, M. Salomé, and R. Bernas, Nucl. Instr. Methods 53, 216 (1967).

[3]B. L. Tracy, J. Chaumont, R. Klapisch, J. M. Nitschke, A. M. Poskanzer, E. Roeckl, and C. Thibault, Phys. Letters 34B, 277 (1971).

[4]L. Yaffe, in *Proceedings of the Second International Atomic Energy Symposium on Physics and Chemistry of Fission, Vienna, Austria, 1969* (IAEA, Vienna, 1969), p. 701. See references cited therein.

[5]J. H. Davies and L. Yaffe, Can. J. Phys. 41, 762 (1963). See also: H. Umezawa, J. Inorg. Nucl. Chem. 33, 2731 (1971).

[6]P. P. Benjamin, D. A. Marsden, N. T. Porile, and L. Yaffe, Can. J. Chem. 47, 301 (1969).

[7]G. B. Saha, I. Tomita, and L. Yaffe, Can. J. Chem. 49, 2205 (1971).

[8]T. D. Thomas and R. Vandenbosch, Phys. Rev. 133, B976 (1964).

[9]A. C. Wahl, A. E. Norris, R. A. Rouse, and J. C. Williams, in *Proceedings of the Second International Atomic Energy Symposium on Physics and Chemistry of Fission, Vienna, Austria, 1969* (see Ref. 4), p. 813.

[10]E. Konecny, H. Gunther, G. Siegert, and L. Winter, Nucl. Phys. A100, 465 (1967).

[11]C. Thibault, Ph.D. thesis, Faculté des Sciences Orsay, 1971 (unpublished).

[12]T. D. Thomas, G. M. Raisbeck, P. Boerstling, G. T. Garvey, and R. P. Lynch, Phys. Letters 27B, 504 (1968).
[13]A. M. Poskanzer, G. W. Butler, and E. K. Hyde, Phys. Rev. C 3, 882 (1971).
[14]L. E. Glendenin, C. D. Coryell, and R. R. Edwards, *National Nuclear Energy Series* (McGraw-Hill, New York, 1951), Div. IV, Vol. 9, p. 489.
[15]R. D. Present, Phys. Rev. 72, 7 (1947).
[16]T. J. Kennett and H. G. Thode, Phys. Rev. 103, 323 (1956).
[17]J. Wing and P. Fong, Phys. Rev. 157, 1038 (1967).
[18]A. C. Wahl, Phys. Rev. 99, 730 (1955).
[19]J. M. Alexander and C. D. Coryell, Phys. Rev. 108, 1274 (1957).
[20]S. H. Freid, J. L. Anderson, and G. R. Choppin, J. Inorg. Nucl. Chem. 30, 3155 (1968).
[21]L. J. Colby, Jr., and J. W. Cobble, Phys. Rev. 121, 1410 (1961).
[22]J. A. McHugh and M. C. Michel, Phys. Rev. 172, 1160 (1968).
[23]J. Chaumont, Ph.D. thesis, Faculté des Sciences Orsay, 1970 (unpublished).
[24]J. P. Cohen, Ph.D. thesis, Faculté des Sciences Orsay, 1968 (unpublished).
[25]I. Dostrovsky, Z. Fraenkel, and P. Rabinovitch, in *Proceedings of the Second United Nations International Conference on the Peaceful Uses of Atomic Energy* (United Nations, Geneva, 1958), Vol. 15, p. 301.
[26]R. Vandenbosch and J. R. Huizenga, in *Proceedings of the Second International United Nations Conference on the Peaceful Uses of Atomic Energy* (United Nations, Geneva, 1958), Vol. 15, p. 284.
[27]E. Cheifetz, Z. Fraenkel, J. Galin, M. Lefort, J. Péter, and X. Tarrago, Phys. Rev. C 2, 256 (1970).
[28]E. Cheifetz and Z. Fraenkel, Phys. Rev. Letters 21, 36 (1968). See also: S. C. Burnett, R. L. Ferguson, F. Plasil, and H. W. Schmitt, Phys. Rev. C 3, 2034 (1971). C. J. Bishop, R. Vandenbosch, R. Aley, R. W. Shaw, Jr., and I. Halpern, Nucl. Phys. A150, 129 (1970).
[29]H. C. Britt and S. L. Whetstone, Jr., Phys. Rev. 133, B603 (1964).
[30]K. Sistemich, P. Armbruster, J. Eidens, and E. Roeckl, Nucl. Phys. A139, 289 (1969).
[31]L. E. Glendenin, H. C. Griffin, W. Reisdorf, J. P. Unik, in *Proceedings of the Second International Atomic-Energy Symposium on Physics and Chemistry of Fission, Vienna, Austria, 1969* (see Ref. 4), p. 781.

PHYSICAL REVIEW C VOLUME 5, NUMBER 1 JANUARY 1972

Neutron Radius of ^{208}Pb from 166-MeV Alpha-Particle Scattering

B. Tatischeff, I. Brissaud, and L. Bimbot
Institut de Physique Nucléaire, 91-Orsay, France

(Received 6 July 1971)

The elastic scattering of α particles is analyzed with an optical potential obtained by a simple folding of the nuclear-matter distribution with an α-nucleon interaction. The ^{208}Pb neutron-matter radius is extracted using the charge-distribution parameters. The result $r_{nm}=5.75\pm0.09$ fm is compared with other determinations and some theoretical calculations.

The proton distribution in nuclei has been obtained from elastic electron scattering or from muonic x-ray spectra. The rms charge radius $r_c=\langle r_c^2\rangle^{1/2}$ and the surface thickness of the charge distributions are relatively well known.[1] The situation is quite different for neutron distributions. If r_p, r_n, and r_{nm} are, respectively, the rms radii of proton, neutron, and neutron-matter distributions, we have $\langle r_p^2\rangle=\langle r_c^2\rangle-0.64$ fm^2 and $\langle r_n^2\rangle=\langle r_{nm}^2\rangle-0.64$ fm^2, the difference corresponding to the nucleon dimension. Different methods have been used for the determination of r_{nm} by means of sometimes questionable approximations. As a consequence, the theoretical results are sometimes inconsistent. The most striking example is that of ^{208}Pb, where the experimental r_{nm} values vary between 5.44 and 6.35 fm. For theoretical calculations, one needs a more precise determination.

The 166-MeV α-particle beam of the Orsay synchrocyclotron was used to measure the elastic scattering differential cross section. It has been shown previously[2-4] that it is possible to calculate an optical potential for 166-MeV α particles which gives a good fit to differential cross sections. The real part of that potential is given by the equation

$$V_{\rm opt}^{\rm R}(r_\alpha)=U_{\rm R}\int V(\vec{r},\vec{r}_\alpha)\rho(\vec{r})d\vec{r}\,, \tag{1}$$

where $\rho(\vec{r})$ is the matter distribution of the nucleus, and $V(\vec{r},\vec{r}_\alpha)$ is an α-nucleon effective interaction obtained from a nucleon-nucleon interaction $V(\vec{r},\vec{r}_\alpha)=V_0\exp\{-[(\vec{r}-\vec{r}_\alpha)/\mu]^2\}$, with $V_0=-37$ MeV and $\mu=2$ fm. For simplicity, the imaginary part of the optical potential is supposed to be proportional to the real part, i.e., $W_{\rm opt}^{\rm I}(r_\alpha)=(U_{\rm I}/U_{\rm R})\times V_{\rm opt}^{\rm R}(r_\alpha)$. It has been shown previously that this